# OBSERVATION OF LOCALIZED DEFORMATION IN PARTIALLY SATURATED SAND BY MICROFOCUS X-RAY CT AND DIC IMAGE ANALYSIS

Yosuke Higo*, Fusao Oka*, Tomohiro Sato**, Yoshiki Matsushima*** & Sayuri Kimoto*
*Department of Civil and Earth Resources Engineering, Kyoto University, Kyoto, Japan
**Former student of Kyoto University, presently in Maruun Kensetsu, Co., Ltd., Niigata, Japan
***Former student of Kyoto University, presently in Central Japan Railway Company, Tokyo, Japan

*Summary* The localized deformation in partially saturated sand has been investigated quantitatively using microfocus X-ray CT and an image analysis of the CT images. Triaxial compression tests on a partially saturated dense sand specimen have been carried out under drained conditions for both air and water. The displacement field has been quantified by the digital image correlation (DIC) technique, through which the progressive development of shear bands has been discussed.

## INTRODUCTION

It is well known that a breakdown in the suction, e.g., by the infiltration of water and/or shearing, induces a large loss in strength involving clearer shear banding with stronger strain softening than fully saturated or dry sand. In the meantime, strain localization, including shear banding, is one of the most important issues in the field of geomechanics, because the phenomenon of strain localization signifies the onset of failure in geomaterials. The aim of this study is to clarify the mechanism of strain localization in partially saturated soil using X-ray computed tomography. X-ray CT has recently been applied to the field of engineering as a powerful tool for viewing the inside of objects in a nondestructive manner. In the last decade, a micro tomography technique has been applied to investigate the microstructures of geomaterials, since the micro CT images with a micron's level of spatial resolution make it possible to observe sand particles individually (e.g., [1]). Recently, the image analysis of CT images by a digital image correlation (DIC) technique has achieved full field measurement, i.e., the quantification of the displacement field (e.g., [2], [3]).
In the present study, the strain localization of partially saturated sand during triaxial compression tests has been discussed through the visualization of the changes in density in the specimen using microfocus X-ray CT and the quantification of the displacement field in the specimen by a DIC image analysis.

## MATERIAL AND METHODS

The test sample used in this study is a type of silica sand called Toyoura sand. Toyoura sand is uniform (the uniformity coefficient is 1.6) and semi-angular in shape with an average diameter $D_{50}$ of 0.185 mm. The dry sand mixed with deaired water was compacted in a mould to be a dense specimen with an initial void ratio of 0.665 and a relative density Dr of 85.9%. The degree of saturation of the specimen was 60.4%. The specimen was put in a thin lucid acrylic cell, which is as transparent against X-rays as possible. A confining pressure of 50 kPa was applied by air pressure without any back pressure. The top and the bottom of the specimen were exposed to the atmosphere. Namely, the air pressure was equal to the atmospheric pressure and the amount of pore water was constant. The axial load was applied through a displacement control system with a constant axial strain rate of 0.5%/min until an axial strain of 20%.
During the triaxial shearing, two types of X-ray CT scanning were performed at axial strain rates of 0% (initial state), 2%, 4%, 8%, 15% and 20%. The microfocus X-ray CT apparatus used in the present study is KYOTO-GEOμXCT (TOSCANER-32250μHDK) [1]. One type is the full CT scan, by which the entire specimen is scanned, and the other type is the partial CT scan, which provides CT images of the partial volume of interest with higher magnification.
Furthermore, the DIC image analysis has been applied to the CT images obtained, in which the translation of the points arbitrarily specified in the reference image to the deformed image is determined by optimizing the cross-correlation coefficient calculated in the correlation window employed around the reference point.

## RESULTS AND DISCUSSIONS

Figure 1(a) shows the vertical cross sections of the full CT images. The two white lines in the vertical cross sections indicate the marker layers of the iron sand. It is seen at the initial state that the colour of the CT image is uniformly light grey. At an axial strain of 2%, the distribution of CT values seems to still be homogeneous. At an axial strain of 4%, it can be seen that the specimen starts to deform to a barrel-like shape and that the central part of the specimen becomes slightly darker, i.e., the density becomes lower than that of the initial state. The lower density regions expand and are localized at an axial strain of 8%, while the localization of the lower density regions becomes clearer and asymmetric at an axial strain of 15%. Finally, it is seen that a clear localization zone develops in the specimen.
The distributions of incremental shear strain are shown in Figure 1(b). The strain levels were provided by adopting the B matrix for the eight-node isoparametric finite elements. The second invariant of incremental deviatoric strain is herein referred to as the shear strain increment. It can be clearly seen that the shear strain localizes with an increase in the axial

strain, and that the localized areas of shear strain correspond to the lower density regions observed in the CT images. Therefore, it can be concluded that shear bands develop in the specimen. In addition, the distributions of shear strain at axial strain levels of 2% and 4% are slightly asymmetric. This means that the preferable inclination of the development of the shear band has been already determined at an axial strain of the peak deviator stress level, whereas the localized deformation in the CT images is not visible at axial strain levels of 2% and 4% and the localization still seems to be symmetric even at an axial strain of 8%.

Partial CT images are shown in Figure 2(a). The location of the partial CT is indicated in the vertical cross section of the full CT image (Figure 1(a)). The voxel size of the partial CT scan is $7.62 \times 12.0$ μm. The DIC technique has been applied to the partial CT images, in which we have applied the two-dimensional DIC to the vertical slice, cross section S-2. In the present analysis, axisymmetric conditions can be assumed before the axial strain reaches 8%, since the asymmetry of the deformation mode is still not significant at this moment. Distributions of displacement vectors are shown in Figure 2(b), in which the displacement vectors with low correlation coefficients have been omitted. It is seen in Case Ap and Case Bp that the left part is displaced in a vertically downward direction, while the central and the right parts are displaced in a horizontally right direction. The transition between the deformation on the right part and that on the left part is rather continuous at this moment. It can be seen in Case Cp that the transition region moves to the right, compared with the former two cases, and that the transition region comes to have a band-like shape whose width is relatively narrow (0.84 mm, roughly 5 times $D_{50}$). This seems to be a bifurcation phenomenon from a continuous deformation to a discontinuous one. This kind of sharp discontinuity is not visible in either the full CT images or the DIC results for the entire specimen at axial strain levels of 4% and 8%. It seems that this kind of narrow shear deformation is one of the reasons for the macroscopic strain softening. Furthermore, it is possible that the breakage of bonding, due to the meniscus water, leads to the shear offset, which is related to the brittle behavior of unsaturated soil.

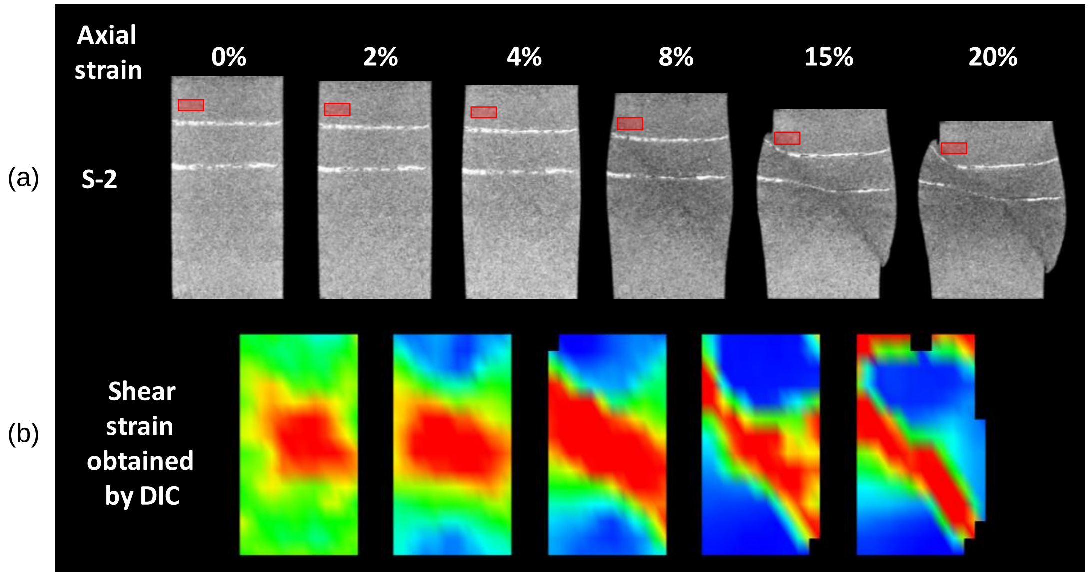


Figure 1 Vertical cross section of the full CT images and the distributions of incremental shear strain obtained by the DIC

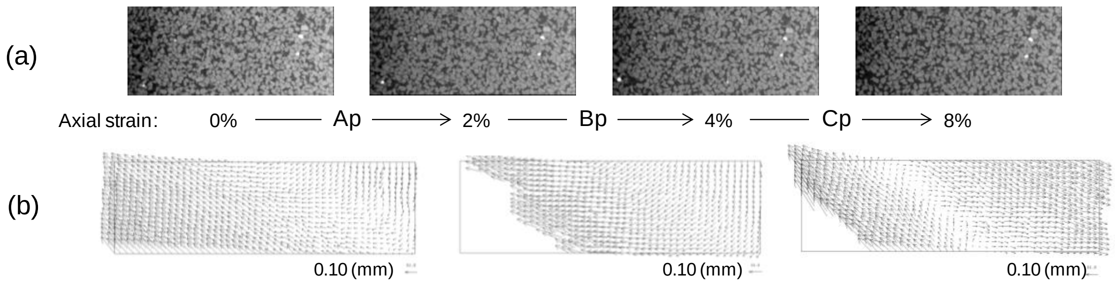


Figure 2 Vertical cross section of the partial CT images and the distributions of incremental displacement vector obtained by the DIC

## References


[1] Higo, Y., Oka, F., Kimoto, S., Sanagawa, T. and Matsushima, Y., Soils and Foundations, 51 (1), pp. 95-111, 2011.

[2] Lenoir, N., Bornert, J., Desrues, J., Bésuelle, P. and Viggiani, G., Strain, 43, pp. 193-205, 2007.

[3] Hall, S.A., Bornert, M., Desrues, J., Pannier, Y., Lenoir, N., Viggiani, G., and Bésuelle, P., Géotechnique, 60 (5), pp. 315-322, 2010.